

MASTER THESIS

# Up to MyLeg with Data

Human Motor Intent Recognition using Multi-Array EMG and Machine Learning

AUTHOR  
R.V. Schulte

DEPARTMENT, FACULTY  
Biomedical Signals & Systems, EEMCS

CHAIR  
prof. dr. J.H. Buurke

EXAMINATION COMMITTEE  
dr. E.C. Prinsen  
M. Sartori, PhD  
prof. dr. ir. P.H. Veltink  
dr. ir. L.J. Spreeuwiers

August 2019



# Summary

During rehabilitation an individual with an amputation learns to perform daily life activities using their prosthesis. A prosthesis, however, is not able to act as a complete replacement of the lost body part. This is partly due to the fact that the prosthesis is limited in intuitive control. Having a prosthesis that can detect an activity before it is performed in combination with a prosthesis that is capable of providing the required torques for this activity could lead to prostheses that are more intuitive. Adding EMG in recognizing movement intent increases performance of such classification algorithms. However, the placement of EMG electrodes over the muscles of interest can be difficult, because the muscle orientation changes as a result of the amputation. Therefore, using multiple electrodes might provide additional spatial information and simplify the placement of electrodes opposed to bipolar EMG. Most classification algorithms are based on features extracted from data, i.e. feature engineering. Instead of manually selecting features, feature learning allows an algorithm to automatically detect points of interest based on raw data. The question arises if either feature learning or feature engineering using unilateral kinematics and multi-array EMG could result in a better performance in terms of intent recognition than using bipolar EMG.

Thirty-five able-bodied subjects (14 male, 21 female) participated in this study. Lower body kinematics as well as 64 EMG channels were recorded. Subjects performed various activities in- and outside the lab to collect more life-like data, including sitting, standing, walking, walking on uneven terrain, walking in confined spaces, turning, stair ascent/descent and ramp ascent/descent. Feature engineering algorithms were based on current state of the art, which consisted of mode-specific linear discriminant classifiers trained on kinematic and EMG features. Feature learning algorithms were based on a convolutional neural network with recurrent layers designed for human activity recognition. Novelty was the use of an ensemble, which combined the output of specifically trained algorithms. Algorithms were trained on several data types: kinematics only, bipolar EMG only, multi-array EMG only, kinematics & bipolar EMG and kinematics & multi-array EMG.

The best overall performing algorithms in feature learning and feature engineering are both based on kinematics & bipolar EMG. This is mainly because the algorithms based on multi-array EMG have poor transition performance. All feature learning algorithms have high steady state performance, but low transition performance. The developed feature engineering algorithm outperformed feature learning in terms of transition ( $p < 0.0001$ ), but the opposite is true for steady-state performance ( $p < 0.0001$ ).

With this research we have gained insight in the possibilities of using EMG and unilateral kinematics to develop an intent recognition system based on machine learning. The feature engineering algorithm based on bipolar EMG and kinematics can easily be implemented in a prosthetic device.

---

# Samenvatting

Tijdens rehabilitatie leren amputatie patiënten om te gaan met hun prothese in het dagelijks leven. Een prothese is alleen niet in staat om het verloren lichaamsdeel compleet te vervangen. Dit komt deels doordat een prothese in mindere mate intuïtief is in gebruik. Een prothese die een activiteit kan detecteren voordat het gebeurt in combinatie met een prothese die de vereiste torque kan leveren bij die activiteit kan leiden tot een prothese die intuïtiever is. Het toevoegen van EMG bij het herkennen van bewegingsintentie verhoogt de prestaties van dergelijke classificatie algoritmes. Het plaatsen van EMG-elektroden over de spieren van interesse kan echter moeilijk zijn, omdat de spieroriëntatie verandert als gevolg van de amputatie. Daarom kan het gebruik van meerdere elektroden aanvullende ruimtelijke informatie bieden en de plaatsing van elektroden in tegenstelling tot bipolaire EMG vereenvoudigen. De meeste classificatie algoritmes zijn gebaseerd op features, karakteristieken in het signaal. Dit wordt feature engineering genoemd. In plaats van het handmatig selecteren van features, stelt feature learning een algoritme in staat automatisch interessante punten te detecteren op basis van onbewerkte gegevens. De vraag is of een feature learning of een feature engineering met behulp van unilaterale kinematica en multi-array EMG zou kunnen leiden tot betere prestaties op het gebied van intentieherkenning, dan het gebruik van bipolaire EMG.

Vijfendertig gezonde proefpersonen (14 mannen, 21 vrouwen) namen deel aan dit onderzoek. Kinematica van het onderlichaam evenals 64 EMG-kanalen op de voor- en achterkant van het bovenbeen werden gemeten. Proefpersonen voerden verschillende activiteiten uit binnen en buiten het laboratorium om meer levensechte gegevens te verzamelen, waaronder zitten, staan, lopen, lopen op oneffen terrein, wandelen in besloten ruimtes, draaien, trap op/aflopen en helling op/aflopen. Feature engineering-algoritmes waren gebaseerd op state-of-the-art, die bestond uit mode-specifieke linear discriminant classifiers die zijn getraind op kinematische en EMG features. Feature learning algoritmes waren gebaseerd op een convolutional neural network met recurrent layers ontworpen voor menselijke activiteitsherkenning. Nieuw was het gebruik van een ensemble, dat de uitvoer van specifiek getrainde algoritmes combineerde. Algoritmes werden getraind op verschillende gegevenstypen: alleen kinematica, alleen bipolair EMG, alleen multi-array EMG, kinematica & bipolair EMG en kinematica & multi-array EMG.

De best presterende algoritmes over het algemeen zijn de algoritmes gebaseerd op kinematica & bipolaire EMG, voor zowel feature learning als engineering. Dit komt vooral omdat de algoritmes gebaseerd op multi-array EMG slechte transitie prestaties hebben. Alle feature learning algoritmes hebben een hoge steady-state prestatie, maar een lagere transitie prestatie. Het ontwikkelde algoritme voor feature engineering presteerde beter dan het feature learning algoritme op het gebied van transitie ( $p < 0.0001$ ), maar het tegenovergestelde is waar voor steady-state prestaties ( $p < 0.0001$ ).

Met dit onderzoek hebben we inzicht gekregen in de mogelijkheden om EMG en unilaterale kinematica te gebruiken om een intentieherkenning methode te ontwikkelen op basis van machine learning. Het feature engineering algoritme op basis van bipolaire EMG en kinematica kan eenvoudig worden geïmplementeerd in een prothese.



# Contents

<b>1</b>	<b>Introduction</b>	<b>1</b>
1.1	Background . . . . .	3
1.2	Goal . . . . .	5
<b>2</b>	<b>Methods</b>	<b>7</b>
2.1	Experimental set-up . . . . .	7
2.2	Data analysis . . . . .	9
2.2.1	Feature engineering . . . . .	10
2.2.2	Feature learning . . . . .	11
2.2.3	Evaluation . . . . .	12
<b>3</b>	<b>Results</b>	<b>15</b>
3.1	Feature engineering . . . . .	15
3.2	Feature learning . . . . .	16
3.3	Engineering versus learning . . . . .	17
<b>4</b>	<b>Discussion</b>	<b>19</b>
4.1	Results . . . . .	19
4.2	Limitations . . . . .	21
4.3	Future Outlook . . . . .	22
<b>5</b>	<b>Conclusion</b>	<b>23</b>
<b>A</b>	<b>Synchronization of EMG and Motion Data</b>	<b>25</b>
A.1	Methods . . . . .	25
A.2	Results . . . . .	27
A.3	Discussion . . . . .	28
A.4	Conclusion . . . . .	28
<b>B</b>	<b>Additional collected data</b>	<b>31</b>
	<b>References</b>	<b>32</b>



# Chapter 1

## Introduction

In the Netherlands alone, more than two thousand patients undergo a major amputation at the lower limb per year [1]. Amputees rehabilitate and learn to perform daily life activities using their prosthesis, although the prosthesis is not able to act as a complete replacement of the lost body part. Most prosthetic devices are passive and can only absorb energy [1]. Furthermore, the movements of the knee are controlled indirectly by using the stump while there is no direct control over the movement of the prosthetic foot. This lack of control makes dynamic balance difficult and makes a prosthesis limited in intuitiveness [1]. The European Horizon 2020 project MyLeg aims at "developing a smart and intuitive osseointegrated transfemoral prosthesis embodying advanced dynamic behaviours" [2]. The project consists of several European partners: University of Groningen, University of Bologna, University of Twente, Roessingh Research & Development (RRD), Radboud University Medical Center (RUMC) and Össur and one Australian partner: Norwest Advanced Orthopedics.

Prostheses that provide power "potentially aid the user in performing tasks that normally require power generation from the amputated leg" [1]. Therefore, the MyLeg prosthesis will be powered. To start the development of the prosthetic device, a list of requirements and needs of the new device was created, based on the experience of three consortium partners with amputees' (RRD, RUMC and Össur), scientific literature and "by holding a workshop with amputees to get their experiences with using prosthetic devices" [1]. It became clear that certain general issues for transfemoral amputees should be the focus for the MyLeg project. Those were (taken from [1]):

1. Impaired balance with increased frequency of stumble and falls.
2. Increased metabolic cost and reduced walking speed.
3. Gait abnormalities
4. Impaired activities of daily living and difficulty with transitions such as sit-to-stand, stairs and uneven terrain.
5. Lack of sensory feedback and intuitive control, and high cognitive load.

To negotiate some of these issues, it has been decided that the prosthetic device requires intent recognition, because intent recognition makes the prosthetic device more intuitive in control. Intuitive control should result in better activity transitions, lower cognitive load and increased balance. A control architecture for the powered prosthetic device has been developed which is shown in figure 1.1. Herein is the high-level control responsible for the intent recognition. The mid and low-level control are responsible for actual control of the actuators and power supply of the prosthesis. Within this mid and low level a state machine is put in place, which controls the actuators to ensure correct biomechatronic behaviour of the prosthetic device during the various gait-related activities. Also the mid level control determines whether transitions are safe and is responsible for acting on sudden movements, such as falls and stumbles.

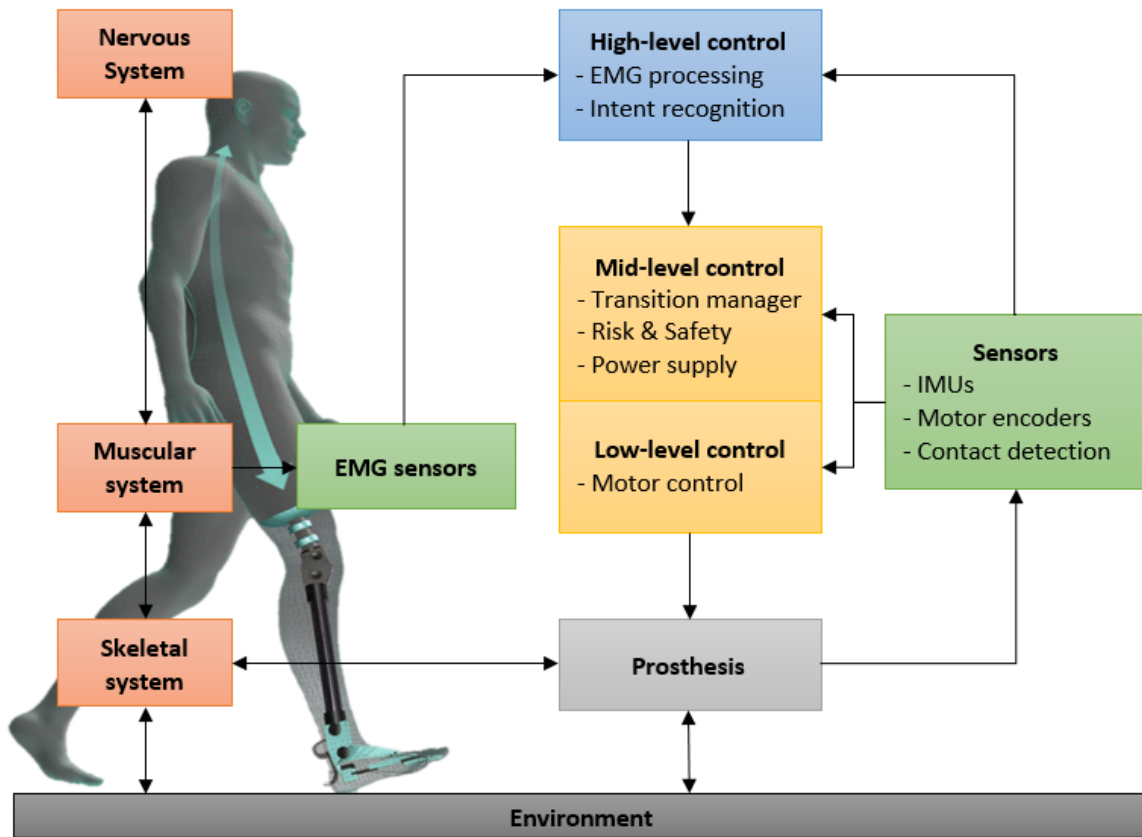


Figure 1.1: Overview of the control architecture of the MyLeg prosthesis.

This thesis was carried out within the work package of the MyLeg project for which RRD is responsible. The work package has been split into the following tasks:

1. Developing a wearable system for the recording of multi-array EMG signals from residual limb muscles.
2. Developing high-level control algorithms in which motor intentions are decoded from the multi-array signals, which will be used to control the prosthetic device.
3. Developing high-level control algorithms in which intramuscular EMG signals will be decoded into motor intentions, which will be used to control the prosthetic device.

This study focuses task 2: high-level control algorithms. The high-level control algorithms should be able to recognize the intent of the following activities [1]:

- Sit-to-stand and stand-to-sit transitions
- Walking on uneven terrain, e.g. grass
- Walking in confined spaces
- Ascending and descending stairs
- Ascending and descending ramps

The algorithms should focus on recognize activities of daily living and transitions in a intuitive way for the user, i.e. the recognizing the intent of the user during daily living. Intent recognition is defined as “using information from the human, assistive device and/or environment detected before movement completion to predict the user’s upcoming locomotor activity” [3].

## 1.1 Background

Human motor intent recognition using electromyography (EMG) has the potential to create intuitive control of prostheses, exoskeletons and other applications [4, 5]. To create intuitive control of a prosthesis, one needs to have a way to detect the intent of the user. Muscle activation can be measured before an action is initiated [6]. In this way the intent of the user can be detected before the activity is performed. Muscle activation as measured using (surface) EMG can therefore be exploited to create more intuitive prosthesis [4].

Currently there are no prosthetic devices commercially available that employ EMG-based intent recognition [7]. However, there are several studies on myoelectric control strategies for the lower limb [7], e.g. [8–13]. Studies have shown that adding EMG in recognizing movement intent increases performance of a classification algorithm, which reduces the error rate and makes the prosthesis more intuitive and reliable [8, 14, 15]. However, the number and placement of electrodes differ per study. In addition, the placement of EMG electrodes over the muscles of interest can be difficult, because the muscle orientation changes as a result of the amputation. Therefore, using multiple electrodes might provide additional spatial information and simplify the placement of electrodes opposed to ‘traditional’ bipolar EMG. Using multiple electrodes in an area is referred to as multi-array EMG or EMG imaging [4]. Instead of measuring one channel per muscle, multiple channels spanning multiple muscles can be measured at once. Combined with other wearable modalities, such as accelerometers and gyroscopes, the amount of data that can be collected with limited effort has greatly increased which enables the decoding of EMG and/or kinematics into motor intent of more complex activities [5, 16, 17].

There are various approaches to recognize motor intent, although most seen in literature is a classification based approach [3, 8–10, 12, 13]. In this approach a window is extracted, e.g. around a gait event such as initial contact. The aim is to recognize or classify the next state the person is in. For instance a person is walking, but after initial contact the person will be ascending stairs. A classifier must be able to recognize this intent to climb stairs based on the information it gets from the window around initial contact. The advantage of using a classification based system is the possibility of using a state machine as control mechanism of the prosthesis, although a state machine has its own limitations, e.g. not able to perform activities that fall outside of the predefined states. In literature other approaches are seen as well, such as proportional or direct control using EMG [11, 18, 19] or using EMG as neural input to human musculoskeletal models [4]. However, in this thesis the focus is primarily on classification based approaches, as the first MyLeg prototype will be controlled with a state machine. Within classification based approaches, two categories can be distinguished: *feature engineering*, which is used in conventional machine learning and *feature learning*, which is used in deep learning [5].

### Feature engineering

Feature engineering is using knowledge of the nature of the signals and reasoning that certain point of interest, so called features, could improve recognition of patterns. In this way useful information is extracted, while unwanted signal and interference can be discarded [20]. Note that the quality and quantity of features are crucial to the performance of the intent recognition [20, 21]. Feature engineering can be performed for any type of biological signal, thus also for kinematics and EMG. In many studies about myoelectric control, e.g. [8, 9], commonly used time domain features in EMG are mean absolute value, waveform length, number of zero crossings and slope sign changes, which were described two decades ago [22]. The current state-of-the-art of gait related motor intent recognition also uses these time domain features [13]. Hu *et al* [13] describe an algorithm where a fusion of EMG and kinematics was used. They have reached an accuracy of 96% using mode-specific Linear Discriminant Analysis (LDA) classifiers. The algorithm used previously described time domain features, together

with sixth order coefficients of an auto-regressive model, which are based on older studies [23, 24]. The time domain features and choice for a LDA classifier seem to work best for EMG related intent recognition [20].

### Feature learning

Instead of manually selecting features, feature learning allows an algorithm to automatically detect points of interest based on raw data. Although using adequate features based on domain knowledge could outperform a feature learning approach, there is a drawback. It "limits a systematic exploration of the feature space" [16], which could lead to a biased and sub-optimal solution. Convolutional Neural Networks (CNNs) are a way to address this problem. CNNs use convolutional layers, where the signal is convoluted with a kernel which is the same as 'regular' filtering. Kernels are small matrices which are 'slid over' a signal during convolution. This enables to recognize patterns which are captured by the kernel. For instance a kernel could be optimized to recognize sharp peaks and when this kernel is convoluted with a sensor channel, all sharp peaks in the signal are emphasized. In the optimization process, these kernels are tuned to extract patterns, i.e. features, that lead to the highest performance. A convolutional layer does not only have one kernel per layer, but multiple, e.g. 64, which results in a 'feature map' with a size of 64. This means that up to 64 different kernels look at the data in different ways and thus extract different kind of features and store them in the resulting maps. Automatic feature selection enables to have more complex features, which is believed to result in better performance to recognize more complex activities [5]. In other domains conventional machine learning based on feature engineering is outperformed by deep learning approaches, such as in image and speech recognition [5, 16].

Ordonez & Roggen [16] applied deep learning to a human activity recognition (HAR) problem. Combining convolutional layers and recurrent layers, which are often used in time series analysis, they managed to outperform conventional machine learning approaches on publicly available data sets [25–27] with their algorithm DeepConvLSTM. The benefit of recurrent layers is incorporating previous information which enables pattern recognition in sequences of data. Long Short Term Memory (LSTM) layers are a type of recurrent layers which are able to 'remember' more information from sequences of data compared to standard recurrent layers. This memory feature makes LSTM layers ideal for temporal data, such as videos or in the case of Ordonez & Roggen, multi-channel sensor information. They were outperformed by an ensemble learning approach by Guan & Plotz [28]. Ensemble learning is learning on output of different classifiers. The idea is to combine classifiers that were trained on different 'views' of the data and hereafter train another classifier, so-called meta-classifier, on the output of the combined classifiers. As the individual classifiers are more 'specialized', combining them results in "more robust and typically better recognizers in terms of classification accuracy" [28]. This gave rise to the idea of an algorithm consisting of classifiers that were trained on specific sensor input, e.g. one classifier for kinematics and one for EMG.

The data sets used for HAR do not contain EMG, but the idea of CNNs can be applied to EMG as well, as demonstrated in upper limb prosthesis control [5]. To our knowledge, deep learning approaches using CNNs and EMG have not been used in motor intent recognition tasks for the lower limb.

## 1.2 Goal

In this thesis two questions will be addressed:

- Could using multi-array EMG in a kinematic driven algorithm result in a higher classification accuracy compared with using bipolar EMG? And furthermore, does EMG have an added benefit at all compared with a base-line kinematic driven algorithm?
- Could deep learning outperform conventional machine learning in terms of performance of recognizing human motor intent?

The goal is to come up with algorithms that could readily be used in a prosthetic device, thus using only information that could be available from sensors within a prosthesis.

### Outline

The thesis consists of several parts, first methods, where experimental set-up, data-analysis and types of algorithms are described. Hereafter results of all different types of algorithms are presented and discussed and concluded in the conclusion. Furthermore, to utilize the collected data, a custom synchronization strategy was developed and validated, see appendix A and additional collected data is described in appendix B.



# Chapter 2

## Methods

### 2.1 Experimental set-up

Data were collected from able-bodied subjects. Subjects were recruited using flyers and convenience sampling. The study and protocols are carried out with the approval of the medical ethical review board of Twente with written informed consent from all subjects.

35 able bodied subjects (14 male, 21 female) participated in this part of the study between March and July 2019. Subjects were  $23 \pm 2$  years,  $179 \pm 9$  cm tall and weighed  $73 \pm 11$  kg. All subjects declared not to have any gait impairments at the time of the measurements.

Lower body kinematics were collected using a MVN Link suit (Xsens, Enschede, The Netherlands), consisting of eight inertial measurement units (IMUs) which were placed on the sternum, lower back (pelvis), both thighs, shanks and feet. 3D acceleration, velocity, position as well as 3D angular velocity and position are recorded per segment at a sample frequency of 240Hz. IMU placement and calibration was performed according to Xsens guidelines [29].

EMG signals were recorded using the Sessantaquattro (Bioelettronica, Turin, Italy) with two EMG grids in a 4x8 configuration and an inter-electrode distance of 10mm at a sample frequency of 2000Hz. EMG was recorded from rectus femoris (RF) and vastus lateralis (VL) at the front of the leg and semitendinosus (ST) and biceps femoris (BF) at the back, see figure 2.1. It was ensured that the one side of the grid was placed on the RF muscle according to the Surface ElectroMyoGraphy for the Non-Invasive Assessment of Muscles (SENIAM) project guidelines [30], and at the back the same for the ST muscle. These four muscles were chosen as they are present in a transfemoral amputee and are responsible for hip flexion (RF) and extension (ST, BF) and knee flexion (VL, RF) and extension (ST, BF). A similar muscle group was targeted in [13]. The electrode configuration is aimed to be used in amputee subjects, where locating the muscle of interest more difficult than in healthy subjects. Therefore, all 64 channels of the Sessantaquattro are used.

Synchronization between Xsens and EMG was performed using an analog accelerometer placed on the right thigh Xsens IMU, using cross-correlation between the acceleration measured by the two different units. Resolution of this method is around 2 ms, see appendix A. To ensure that time stamps corresponded between kinematics and EMG, all data were resampled to 1000Hz.

To have more life-like data, measurements were conducted partly in a lab, but also outside. All measurements took place in and around Roessingh Research & Development, Enschede, The Netherlands. Each subject performed five types of trials in the same order:

- **Uneven terrain** A trial consisted of sitting on a bench, standing up, walking on level ground, walking on grass, standing still and walking back and sitting down, see figure 2.2a.
- **Stairs** Subject sat on a stair, stood up, ascended two flights of stairs, one consisting of eleven steps, the other of nine steps. Hereafter the subject stood still, turned around and descended

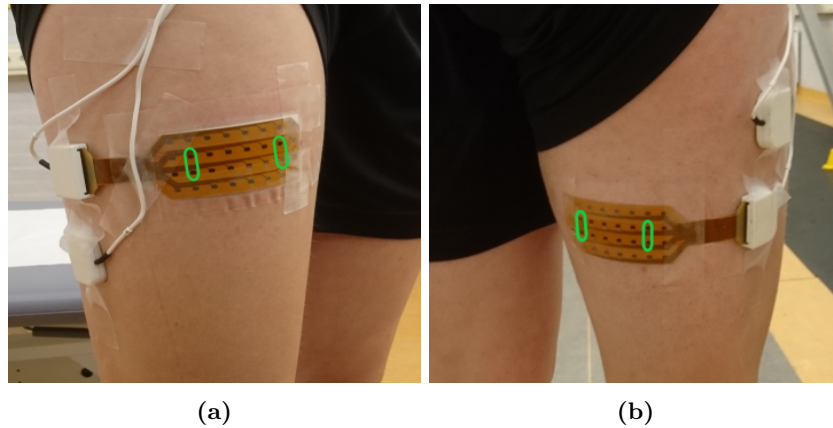


**Figure 2.1:** Placement of EMG grids on the (a) front and (b) back of the leg. Green ovals indicate selected electrodes for bipolar EMG.

the stairs and finally sat down again, see figure 2.2b.

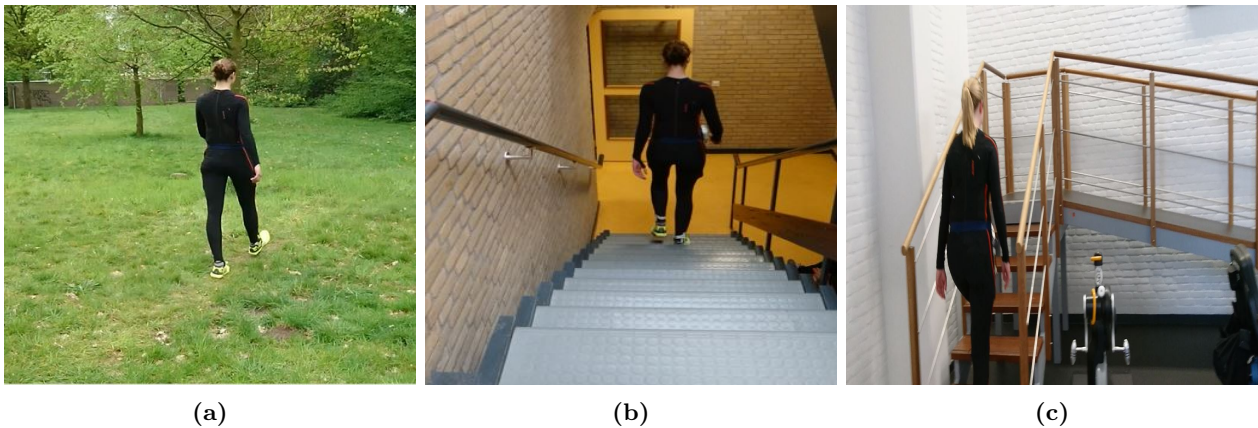


**Figure 2.2:** (a) Walking on grass, (b) one out of two flights of stairs subjects had to ascent and descent, (c) stairs and ramp combination, which also needed to be ascended and descended by subjects.

- **Ramp** The trial started with ascending a staircase with seven steps, reaching a plateau and descending a ramp (10 degrees) which continued into a steeper ramp (15 degrees) after three meters. The subject stood still at the end of the ramp, turned around and ascended the ramp. Hereafter the subject descended on the stairs and turned around to start the trial again, see figure 2.2c.
- **Uneven terrain II** This path consisted of uneven terrains found in the street. First the subject needed to come over a speed bump and hereafter walk on level ground towards the first type of uneven terrain. This terrain consisted of small square stones which were slightly uneven. The subject crossed this terrain and walked onto the terrain consisting of unevenly laid Belgian blocks. After passing this terrain, the subject turned around and walked back over all types of terrains and repeated the trial, see figure 2.3a.
- **Confined spaces** The subject lay on a bed, stood up and walked towards confined spaces set-up. The subject took small steps in all directions, i.e. forwards, backwards, sidesteps to left or right, diagonally forwards, backwards to either left or right, see figure 2.3b.

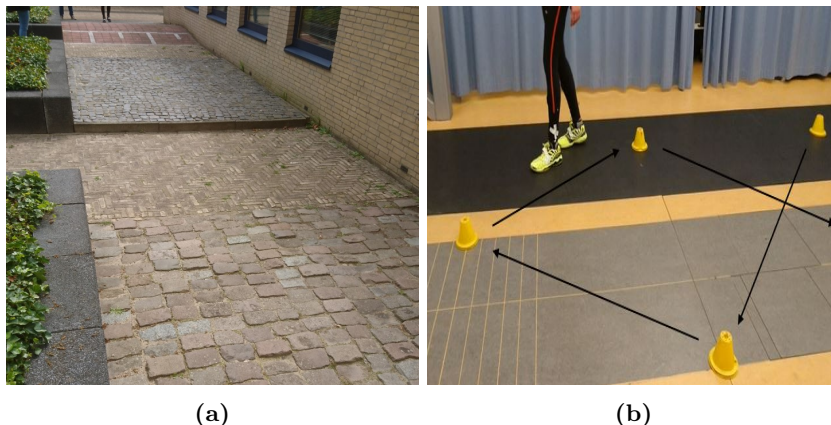


**Figure 2.3:** (a) Uneven terrain II, where the trial started with a speed bump at the top of the image and hereafter two types of uneven terrain, (b) confined spaces set-up within the lab.

Between the trials the subject walked to each location and this data were recorded as well. Each trial was conducted ten times, with a total measurement time of around two hours, including subject preparation, sensor placement and calibration.

## 2.2 Data analysis

Kinematic data used in analysis of each subject included 3D acceleration and angular velocity of the right foot, lower and upper leg and the joint angles of the right ankle and knee. These variables were chosen to have data which could be extracted from a prosthesis, without the need of additional kinematic sensors on the body itself. Although force and torque sensors are probably available within a prosthesis, these are not taken into account due to the difficulty of measurement outside a lab environment. All EMG channels were recorded in a monopolar fashion. Four pairs of channels were selected by evaluating the position of the electrode grid on the subject. Each pair of signals was subtracted from itself and this represented the regular bipolar EMG. The 32 channels in front and 32 channels at the back of the leg were filtered in spatial direction using the normal double differential (also called Laplacian) which is commonly used for EMG electrode grids [4]. Those 64 filtered channels are referred to as multi-array EMG from now on. This means that both multi-array and bipolar EMG from the same subject during the same measurement was available. EMG data was filtered with a zero-lag second order Butterworth band-pass filter between 20 and 450Hz. Ten labels were considered. These were non-weight bearing (sitting and lying down, which is called sitting from now on), standing, turning, walking, stair ascent & descent, ramp ascent & descent, uneven terrain (all types) and confined spaces. As walking on uneven terrain is similar to walking, uneven terrain was labelled as walking as well to see its effect.

Initial tests showed that the sliding window approach, as in [16], was not feasible in correctly recognizing transitions, where as the gait event based approach, as used in [13] showed better initial results. Therefore, data was split in 256 ms windows around initial contact for gait related activities. Initial contact was determined using peak foot acceleration. For non gait related activities, such as sitting, the windows were just before a transition of one state to the next and between transitions. All algorithms, which are described below, consisted of mode-specific classifiers as in [13]. This means that each classifier was trained on a specific activity and the classifiers were restricted that no ‘forbidden’ transition could take place, e.g. stair ascent could stay in stair ascent state or could transition to level-ground walking, but not to ramp descent, see table 2.1. The window size was slightly shorter than [13], where 300 ms windows were used. Using a windows size with a size with base 2, reduces

**Table 2.1:** Possible transitions and their occurrence in percentage. The blank spaces indicate the forbidden transitions. E.g. standing to ramp descent is a allowed transition, although it does not occur in the data (0.0%).

To \ From	Sitting	Standing	Walking	Turning	Stair Asc.	Stair Dsc.	Ramp Asc.	Ramp Dsc.	Uneven T.	Conf. spaces
Sitting	80.3	19.7								
Standing	5.8	66.3	5.3	10.7	1.9	2.3	3.7	0.0	3.7	0.3
Walking		12.0	45.5	2.1	10.3	5.8	3.3	8.7	9.5	2.9
Turning		32.5	0.0	67.5					0.0	
Stair Asc.		6.2	11.3		82.5					
Stair Dsc.		6.9	18.2			74.9				
Ramp Asc.		0.3	17.2				82.5			
Ramp Dsc.		14.4	9.0					76.6		
Uneven T.		6.0	12.6	2.0					79.4	
Conf. spaces		0.3	2.3							97.4

training time on a GPU. Therefore, a window size of 256 ms is used instead of 300 ms. This had no effect on performance during initial tests.

All evaluation was done offline using python 3.6 with the packages scikit-learn for the feature engineering algorithms and keras with tensorflow back-end [31] for the feature learning algorithms.

### 2.2.1 Feature engineering

The algorithm is based on the work of Hu *et al* [13], where a fusion of EMG and kinematics was used as described before. Important to note is that they had only included level-ground walking, stair ascent/descent, ramp ascent/descent. As their data set is publicly available [32], it enabled to recreate their method, validate it on their data set and apply it to our own data set. It should be noted that our data set only contained EMG from the RF, VL, ST and BF. Furthermore, our data set contained more types of activities and were not performed in as standardized circuits as Hu *et al*. IMU and joint angle data is comparable.

The algorithm existed of multiple linear discriminant analysis classifiers (LDA), which were trained per mode (i.e. state). This means the algorithm used the incoming state to chose the LDA classifier corresponding to that incoming state. This classifier was trained on data that only corresponded with that incoming state. With ten different states, ten LDA classifiers were trained per algorithm. Features were extracted from each window. Six features were extracted for each kinematic channel, which were mean, standard deviation, maximum, minimum, initial and final value [13]. For each EMG channel, ten features were extracted. Those were mean absolute value, waveform length, number of zero crossings and slope sign changes, and the coefficients of a sixth-order auto-regressive model [13]. This means that per window there are 120 kinematic features and 40 bipolar EMG features, where as for multi-array EMG there are 640 features. All features are normalized to have zero mean and unit variance, in accordance with Hu *et al* [13].

Other than the window length, there were other deviations from the algorithm by Hu *et al*. During initial testing using principal component analysis (PCA) preserving 95% of the variance did not improve the results and was left out. Furthermore, the original algorithm was trained on toe-offs and initial contacts. Due to inaccuracies in toe-off determination, only initial contacts were used. Thus the algorithm needed to determine the state of the activity after initial contact or selected window during the non-gait cycle activities. As the data was biased towards staying in the same state, i.e. steady-state, performance on transitions was poor. Therefore, two classifiers were trained per mode, one for the steady-state and one for the transitions. The transition classifier was trained on the same data with one alteration. For each mode the occurrence was determined, see table 2.1, and the transition states were weighted by a factor ten, which emphasizes the transition. During testing, the classifier

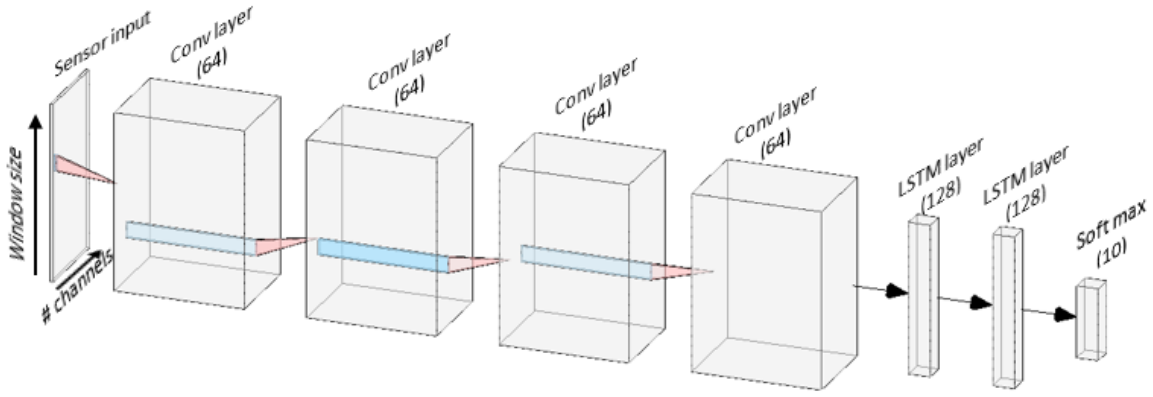


**Figure 2.4:** Feature learning architecture. Herein is ‘conv’ a convolutional layer and the number (64) indicates the number of channels. Probability estimates for each class comes from the final soft max layer.

which had the highest probability, i.e. which one was most certain, was chosen to determine the mode.

## 2.2.2 Feature learning

This algorithm is based on the work of Ordonez & Roggen [16]. The algorithm consisted of multiple mode specific classifiers which consisted of four convolutional layers which acted as ‘feature extractors’ and two long short term memory (LSTM) layers to model temporal information and one dense soft-max layer which acted as the ‘interpreter’, see figure 2.4. Each 2D convolutional layer consisted of 64 kernels and were applied per sensor channel with a kernel size of 5 by 1. The rectified linear unit was used as activation function in each convolutional layer. Each LSTM layer contained 128 units and uses the same activation functions as described by Ordonez & Roggen. Each classifier was trained using RMSprop with a learning rate of 0.001.

Novelty in this feature learning algorithm was the use of an ensemble. Guan & Plotz [28] described in depth how to combine the output of multiple classifiers. A classifier was trained on each category of data, i.e. kinematics only, EMG only or a combination of kinematics & EMG. The output of each classifier  $m$  is a probability vector  $\mathbf{p}_t^m$  for each point in time  $t$ . The vectors of all models  $M$  are combined using the mean and results in the final score vector  $\mathbf{p}_t^{ensemble}$ :

$$\mathbf{p}_t^{ensemble} = \frac{1}{M} \sum_m^M \mathbf{p}_t^m \quad (2.1)$$

The class with the highest probability represents the predicted class. To compare performance, a feature learning algorithm using all sensor input was trained as well, see figure 2.5a.

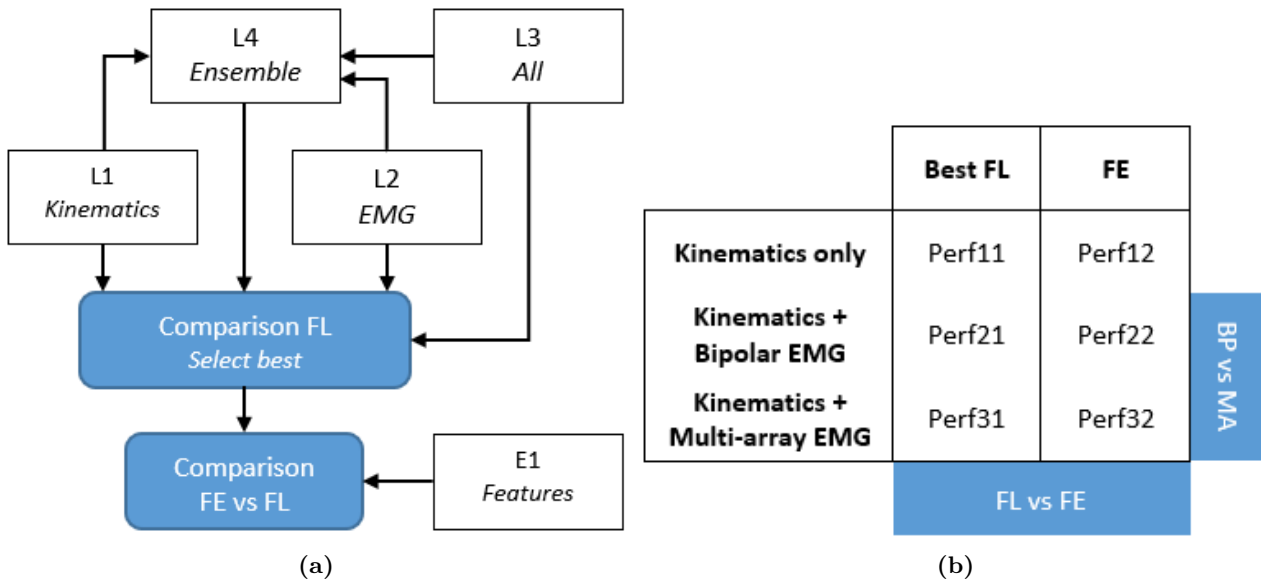


**Figure 2.5:** Evaluation of the various algorithms. (a) Selection of the best feature learning (L1-4) algorithm to compare against the feature engineering algorithm (E1). Type of sensor input is stated in italics. The output of algorithms L1-3 are used in algorithm L4, the ensemble. (b) All types of algorithms are trained on kinematics and on either bipolar EMG or multi-array EMG and two comparisons are made: FL vs FE and bipolar (BP) vs multi-array (MA) EMG. Furthermore, algorithms without EMG (kinematics only) are trained to give a base-line performance.

### 2.2.3 Evaluation

Three things needed to be compared: First the best feature learning algorithm had to be selected. Hereafter the best performing feature learning algorithm was compared against the feature engineering algorithm. For clarification, see figure 2.5. All algorithms were trained on kinematics and on one of the two different types of EMG, bipolar or multi-array EMG, to see if multi-array enhances performance compared with bipolar EMG. To confirm the benefit of EMG in general, a kinematics only algorithm is trained as well.

The performance is represented as accuracy, which is the fraction of correctly classified samples. This performance is also split into steady state performance, i.e. remaining in the same state and transitional performance, i.e. going from one state to the other.

All classifiers were validated with the same window lengths using the same five-fold cross validation. Each validation set contained all types of activities. Both feature learning algorithms and feature engineering algorithms were trained on subject specific data, see figure 2.6. However, before subject-specific training, the feature learning algorithms were trained on data of all other subjects, whereas feature engineering algorithms were not. During initial testing these settings yielded the best results. This training and validation process was repeated for each data type: kinematics, kinematics & bipolar EMG and kinematics & multi-array EMG. Feature learning algorithms also were trained on bipolar EMG only and multi-array EMG only and combined with other algorithm outputs to form the ensemble, see figure 2.5a. To determine the best performing feature learning algorithm a repeated measures ANOVA with Bonferroni correction was performed. Hereafter feature learning and feature engineering algorithms were compared with a paired t-test.

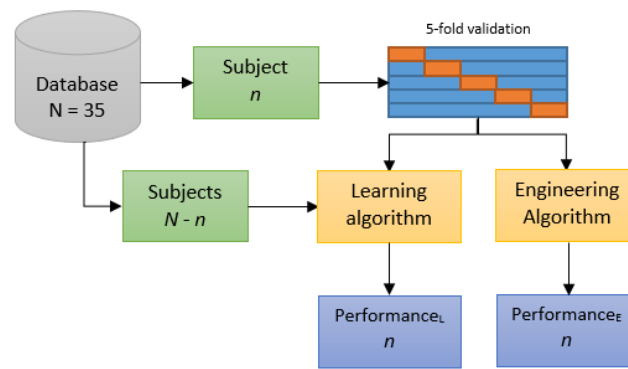


**Figure 2.6:** Overview of training and validation strategy. For each subject  $n$  a five-fold cross validation is performed, which means 80% of the data is in the training set (blue) and 20% in the validation set (orange). The training set for the learning algorithm was further enlarged with all remaining subjects. Performance is thus determined per subject per type of algorithm and is the average performance of the cross fold validation.



# Chapter 3

## Results

All algorithms were trained as aforementioned. First an overview is given per type of algorithm to compare the type of data that was used and hereafter algorithms were compared. For all statistical analyses normality was visually confirmed. Results are reported as average error rate (1-performance) with the standard error of the mean (SEM).

### 3.1 Feature engineering

Performance is shown in figure 3.1 expressed as the error rate (1-performance) for clarity. Looking at overall performance, the algorithm using kinematics and bipolar EMG (KIN+BP) outperforms the algorithm using kinematics only (KIN) and kinematics with multi-array EMG (KIN+MA) significantly ( $p < 0.001$ ). In terms of steady-state performance KIN+MA outperforms KIN and KIN+BP ( $p < 0.0001$ ) and KIN+BP outperforms KIN ( $p < 0.0001$ ). Looking at transition performance KIN+MA is outperformed by KIN and KIN+BP ( $p < 0.0001$ ). All significant differences between the classifiers are the same when uneven terrain is included as a different state or uneven terrain is labeled as walking. Uneven terrain labeled as walking increases performance.

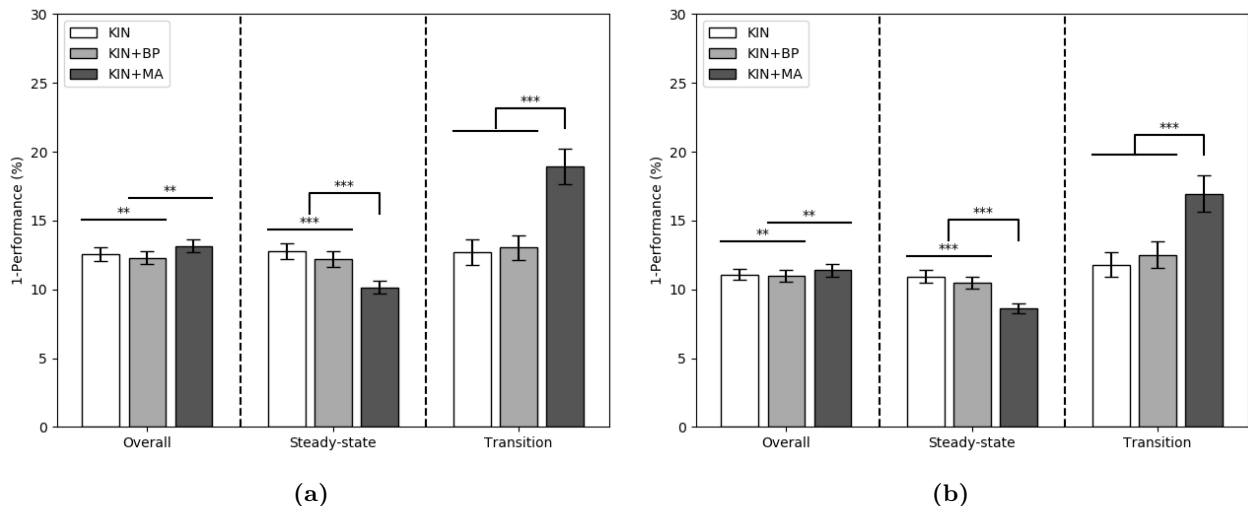


**Figure 3.1:** Average error rate (1-performance)  $\pm$  SEM of feature engineering algorithms in terms of overall, steady state and transition performance, trained on kinematics (KIN) only, kinematics & bipolar EMG (KIN+BP) or kinematics & multi-array EMG (KIN+MA), (a) with uneven terrain, (b) uneven terrain labeled as walking. Stars indicate significance level: \* =  $p < 0.05$ , \*\* =  $p < 0.01$ , \*\*\* =  $p < 0.001$ , etc.

Confusion matrices are shown in figures 3.2a & 3.2b. Most errors occurred where the algorithm predicts standing instead of the activity, e.g. standing instead of turning (24.8% of the cases). Another cause of error is that uneven terrain is confused with walking (13.3% of the cases).

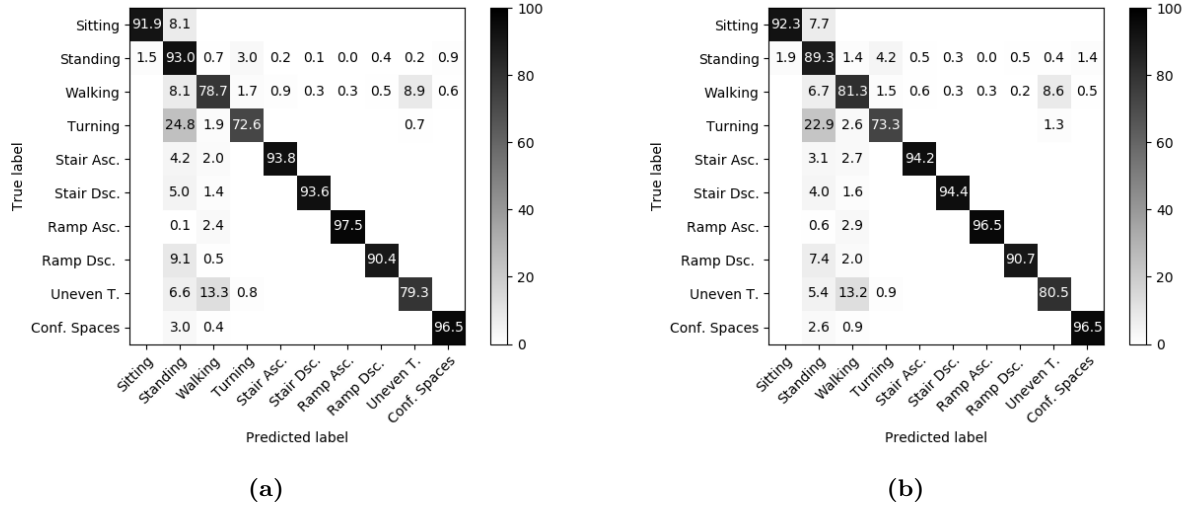


**Figure 3.2:** Confusion matrices of (a) algorithm using kinematics and bipolar EMG (KIN+BP) and (b) algorithm using kinematics and multi-array EMG (KIN+MA). The matrices are normalized over the rows and presented as percentage.

### 3.2 Feature learning

Performance is shown in figure 3.3 expressed as the error rate (1-performance) for clarity. The performance of the EMG only algorithms are not shown in the figures, as the performance was significantly worse than the other algorithms ( $p < 0.0001$ ) and would have made the differences between other algorithms unclear. The average performance of the EMG only algorithms was 73.4%/87.0%/49.2% (overall/steady-state/transition performance) using bipolar EMG and 72.3%/86.2%/47.6% using multi-array EMG. No significant difference was found between the two EMG only algorithms ( $p > 0.05$ ).

In figure 3.3a performance is shown where uneven terrain is included as separate label. Looking at overall performance, the ensemble algorithm using kinematics and bipolar EMG (ENS\_BP) outperforms the algorithm using kinematics only (KIN) and the algorithm trained on kinematics and bipolar EMG (ALL\_BP) significantly ( $p < 0.01$ ). The algorithm trained on kinematics and multi-array EMG (ALL\_MA) is outperformed by ENS\_BP and ALL\_BP ( $p < 0.0001$ ) and by the ensemble algorithm using kinematics and multi-array EMG (ENS\_MA) significantly ( $p < 0.0001$ ). Looking at steady-state performance, ENS\_BP outperforms KIN, ALL\_BP and ALL\_MA ( $p < 0.0001$ ). ENS\_MA outperforms KIN, ALL\_BP and ALL\_MA ( $p < 0.0001$ ). In terms of transition performance ALL\_BP outperforms ALL\_MA and ENS\_MA ( $p < 0.0001$ ). ENS\_MA is outperformed by KIN and ENS\_BP ( $p < 0.001$ ).

In figure 3.3b the performance is shown where uneven terrain is labeled as walking. Looking at overall performance, ALL\_MA is outperformed by KIN, ALL\_BP and ENS\_BP ( $p < 0.001$ ). ENS\_BP outperforms ENS\_MA ( $p < 0.01$ ). Looking at steady-state performance ENS\_BP outperforms KIN ( $p < 0.01$ ), ALL\_BP ( $p < 0.001$ ) and ALL\_MA ( $p < 0.0001$ ). ENS\_MA outperforms ALL\_MA ( $p < 0.0001$ ). Looking at transitions ALL\_BP outperforms ENS\_BP, ALL\_MA and ENS\_MA ( $p < 0.0001$ ).

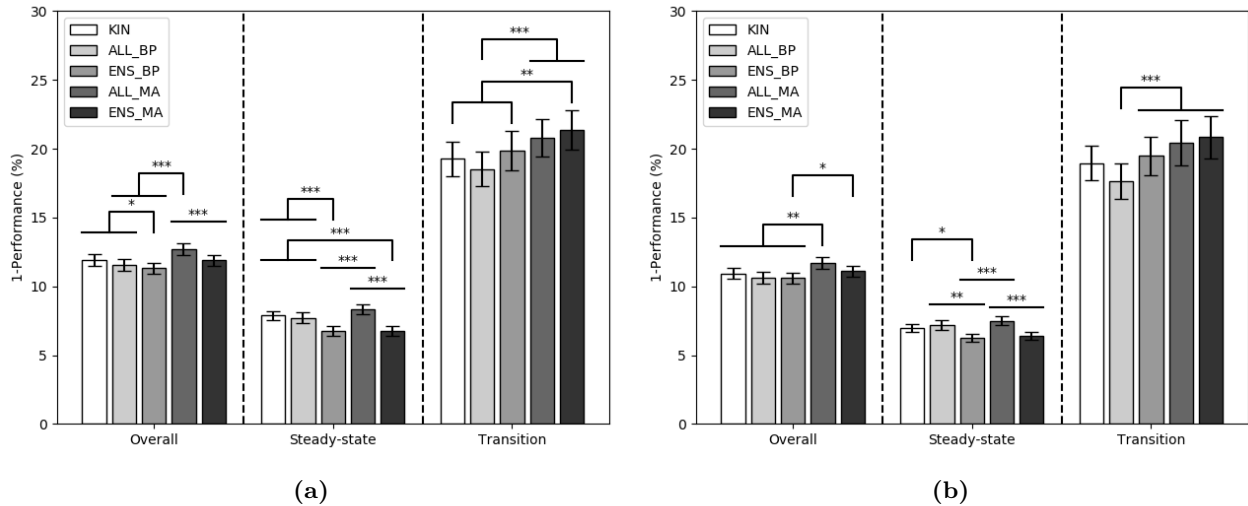


**Figure 3.3:** Average error rate (1-performance)  $\pm$  SEM of feature engineering algorithms in terms of overall, steady state and transition performance, trained on kinematics (KIN), on kinematics & EMG (ALL) or as ensemble (ENS) with either multi-array EMG (MA) or bipolar EMG (BP), (a) with uneven terrain, (b) uneven terrain labeled as walking. Stars indicate significance level: \* =  $p < 0.01$ , \*\* =  $p < 0.001$ , etc.

### 3.3 Engineering versus learning

Performance of the best feature learning algorithms and feature engineering algorithms are shown in tables 3.1a & 3.1b. Best feature learning algorithms are considered to be ALL\_BP using bipolar EMG and ENS\_MA using multi-array EMG.

Looking at table 3.1a where uneven terrain was included as label. No significant differences were found between the feature learning (FL) and engineering algorithms (FE) looking at overall performance ( $p > 0.05$ ). FL outperforms FE in terms of steady-state performance ( $p < 0.001$ ). FE outperforms FL ( $p < 0.001$ ) in terms of transition performance, except for kinematics + multi-array EMG ( $p > 0.05$ ).

Looking at table 3.1b where uneven terrain was labeled as walking. No significant differences were found between FL and FE looking at overall performance ( $p > 0.05$ ). FL outperforms FE in terms of steady-state performance ( $p < 0.001$ ). FE outperforms FL in terms of transition performance ( $p < 0.05$ ).

Figures 3.4a and 3.4b show the performance of the best feature engineering and feature learning algorithms. Both feature engineering as feature learning algorithms were trained on kinematics and bipolar EMG (KIN+BP and ALL\_BP). No significant differences were found between feature learning and feature engineering algorithms ( $p > 0.05$ ). Feature learning outperforms feature engineering ( $p < 0.0001$ ) in terms of steady-state performance. Feature engineering outperforms feature learning ( $p < 0.0001$ ) in terms of transition performance.

**Table 3.1:** Average performance  $\pm$  SEM of best feature learning (FL) algorithm versus feature engineering (FE) algorithm in percentage with p-value, (a) with uneven terrain (UT), (b) with uneven terrain labeled as walking. Red p-value indicates no significant difference with  $\alpha = .05$ .

<i>UT</i>	Overall			Steady state			Transition		
	<i>FL</i>	<i>FE</i>	<i>p</i>	<i>FL</i>	<i>FE</i>	<i>p</i>	<i>FL</i>	<i>FE</i>	<i>p</i>
<b>Kinematics only</b>	88.1 $\pm$ 0.4	88.4 $\pm$ 0.4	0.600	92.1 $\pm$ 0.4	88.4 $\pm$ 0.4	<1e-3	80.7 $\pm$ 1.3	88.0 $\pm$ 0.7	<1e-3
<b>Kinematics + Bipolar EMG</b>	88.5 $\pm$ 0.4	88.6 $\pm$ 0.4	0.860	92.3 $\pm$ 0.3	89.0 $\pm$ 0.4	<1e-3	81.5 $\pm$ 1.3	87.3 $\pm$ 0.7	<1e-3
<b>Kinematics + Multi-array EMG</b>	88.1 $\pm$ 0.4	87.6 $\pm$ 0.4	0.380	93.2 $\pm$ 0.3	90.4 $\pm$ 0.4	<1e-3	78.6 $\pm$ 1.5	82.1 $\pm$ 1.1	0.064

(a)

<i>UT as walking</i>	Overall			Steady state			Transition		
	<i>FL</i>	<i>FE</i>	<i>p</i>	<i>FL</i>	<i>FE</i>	<i>p</i>	<i>FL</i>	<i>FE</i>	<i>p</i>
<b>Kinematics only</b>	89.0 $\pm$ 0.4	89.7 $\pm$ 0.3	0.220	93.1 $\pm$ 0.3	90.1 $\pm$ 0.3	<1e-3	81.0 $\pm$ 1.3	88.8 $\pm$ 0.7	<1e-3
<b>Kinematics + Bipolar EMG</b>	89.4 $\pm$ 0.4	90.0 $\pm$ 0.3	0.234	92.8 $\pm$ 0.3	90.7 $\pm$ 0.3	<1e-3	82.4 $\pm$ 1.3	88.3 $\pm$ 0.7	<1e-3
<b>Kinematics + Multi-array EMG</b>	88.9 $\pm$ 0.4	89.3 $\pm$ 0.4	0.482	93.6 $\pm$ 0.3	92.0 $\pm$ 0.3	<1e-3	79.2 $\pm$ 2.0	83.9 $\pm$ 1.1	0.043

(b)

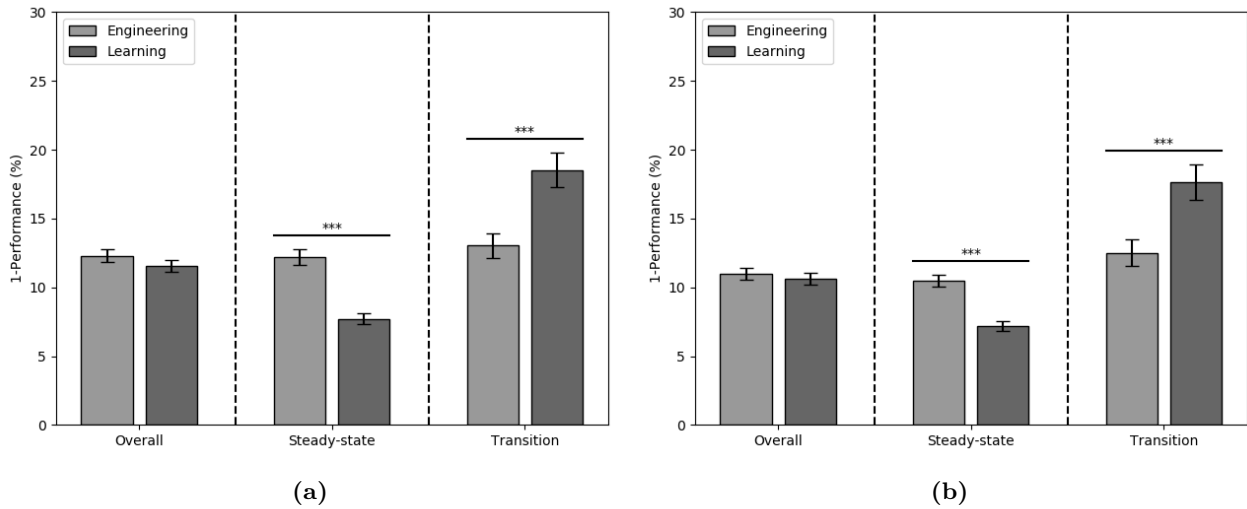


**Figure 3.4:** Average error rate (1-performance)  $\pm$  SEM of the best feature engineering algorithm versus the best learning algorithm in terms of overall, steady state and transition performance, trained on kinematics & bipolar EMG (a) with uneven terrain, (b) uneven terrain labeled as walking. Stars indicate significance level: \* =  $p < 0.01$ , \*\* =  $p < 0.001$ , etc.

## Chapter 4

# Discussion

This study had several goals. First, to investigate whether the use of multi-array EMG in kinematic driven algorithms for human motor intent recognition outperforms algorithms using bipolar EMG and whether EMG has added benefit at all in terms of performance. Second, to investigate whether deep learning outperforms conventional machine learning in terms of human motor intent recognition. To investigate these goals an extensive data set was collected where lower-limb kinematics and EMG were measured simultaneously. Measurement set-up was completely wearable which allowed measurements outside a standardized lab environment. Standard ways of continuous synchronization, e.g. measuring a pseudo random signal simultaneously on two measurement systems, could not be used, as the motion capture system did not allow recording of additional analog signals. Therefore, a custom synchronization method was successfully developed and validated to synchronize kinematics and EMG. Furthermore, state-of-the-art algorithms were implemented and trained on various types of data which the data set contained, to see which strategy would perform best in terms of human motor intent recognition.

### 4.1 Results

Looking at the feature engineering results, it can be concluded that the algorithm using kinematics and bipolar EMG outperformed the other two algorithms ( $p < 0.001$ ). This was mainly because the algorithms based on multi-array EMG had poor transition performance. The algorithms based on multi-array EMG had difficulty to find the relation between the signals and the intent. One explanation for this is that 64 channels measured only four muscles. Per muscle only one signal would be enough, as the additional spatial information was limited. This caused redundancy in the data, where an algorithm struggles to see the cohesion between input and output. Bipolar EMG on the other hand was more ‘focused’ data, with one signal per muscle, which enabled easier recognition. The steady-state performance of the algorithm using kinematics and multi-array EMG however, outperformed the other two algorithms ( $p < 0.0001$ ). This can be explained by that when an algorithm is uncertain, it tends to go for the majority class. As the majority of the data is remaining in the same state, the algorithm can take “the easy way out” and predicts to remain in the same state most of the time. This resulted in a high steady-state performance, but low transition performance. Therefore, it is important to not only report an overall performance, but also steady-state and transition performance when reporting results for intent recognition algorithms. This does not mean that transition performance is more important than steady-state performance. An algorithm with perfect transition performance but worse steady-state performance is not ideal. This would mean that the algorithm predicts transitions constantly, e.g. predicting stair ascent while the user is walking. The user does not benefit from the predictions the algorithm makes in that case. It is therefore important that a good trade-off is chosen between

steady-state and transition performance.

Looking at feature learning algorithms, using bipolar EMG resulted in a higher performance than using multi-array EMG. While this was also the case in the feature engineering algorithms, this was not expected for feature learning algorithms. Feature learning might find relations which are not be found in conventional machine learning. Therefore, feature learning outperforms pattern recognition strategies in the domain of image recognition. However, large data sets are necessary to reach adequate performance. During initial testing on a smaller subset of the data (around ten subjects), overall performance around 80% were found for the deep learning algorithms. Now with all thirty-five subjects included, performance was around 88%. This means that increasing the data set will possibly increase performance for feature learning algorithms. Using ensembles did not give the expected result in terms of performance. The idea behind it was that combining more specialized algorithm would result in higher accuracy. Unfortunately this was not the case. Possibly due to the poor transition performance of the EMG only algorithms, the transition performance of the ensemble worse than its 'all' counterpart. However, the differences for multi-array EMG based algorithms, ENS\_MA and ALL\_MA were small in terms of transition. The ensemble did outperform its counterpart in terms of overall and steady-state performance. Therefore, the ensemble might have added benefit in terms of performance for the algorithms based on multi-array EMG.

Comparing feature learning and engineering, it can be seen in figure 3.4 that the algorithms did not differ significantly in terms of overall performance ( $p > 0.05$ ). Feature engineering had comparable performance looking at overall, steady-state and transition performance. Feature learning had a better steady-state performance ( $p < 0.0001$ ) but worse transition performance ( $p < 0.0001$ ). Looking at all feature learning algorithms, it can be said that feature learning algorithms have high steady state performance, but low transition performance. One explanation is similar as before: the data contains primarily steady states, i.e. the probability of staying in the same state is higher than the probability of transitioning to a different state. The lack of data might have resulted in poor performance by the feature learning algorithms, as there were not enough samples to learn from. Another reason is that the transitions from one state to the next were not standardized. Subjects were free to use whichever leg they preferred, whereas amputees have a preference to use their non affected side first when transitioning from walking to climbing stairs for instance. The feature engineering did not suffer as much from this issue, as it requires less data to perform well. It is expected that both feature learning as feature engineering algorithms will perform better if they are trained on more standardized transitions, e.g. always turning in same direction or starting to climb stairs with the same leg. Especially turning was often confused with standing (see figure 3.2), as one could stand still with one leg and start turning with the other, the algorithm had a difficult time distinguishing those classes.

Comparing the algorithms using kinematics and EMG and the algorithms using kinematics only, it can be seen that the performance did not differ much from each other. For example the best performing feature engineering algorithm using bipolar EMG (KIN+BP) performed significantly better than its kinematics only counterpart (KIN) ( $p < 0.001$ ). However, the difference in average overall performance was small: 88.6% versus 88.4% for KIN+BP and KIN respectively. One could argue that using EMG in this set-up is not as beneficial as expected. Placement of electrodes is additional work an user has to perform, but gets only a minor improvement in performance. This might suggest that the EMG signals derived in this set-up from four upper leg muscles do not provide enough additional information about intent.

## Related works

The feature engineering algorithm was based on the work of Hu *et al* [13], which was in turn based on the works of Young *et al* [8] and Spanias *et al* [15]. Hu *et al* measured on healthy subjects as well and reported a performance of 97.9%/99%/94.9% for overall/steady-state/transition performance for the ipsilateral sensor set-up. They also showed that using their intent recognition system had similar performance for a transfemoral amputee with a experimental prosthetic device. Another conclusion was that using bilateral sensors, the performance of the intent recognition system was significantly better [12, 13]. However, it is considered to be beneficial if the user of the amputee does not require additional sensors on the health leg, thus a ipsilateral sensor set-up is preferred in this thesis.

Other research groups implemented intent recognition systems based on EMG in their experimental prosthetic devices. Fluit *et al* described all available prosthetic devices with intent recognition based on EMG up to now [7]. It can be seen that overall accuracy varies from 89 to 100%. However, most seen activities were walking, ramp ascent/descent and stair ascent/descent. Sometimes standing and sitting were considered as well. This limited set of activities made it difficult to compare accuracy with this thesis' result. Usually only certain transitions were allowed, for instance stand to walk, walk to ascent, but not stair ascent to stand. In this thesis more transitions were allowed to more possible states, which resulted in lower overall accuracy. It can be seen in the confusion matrices of figure 3.2 that standing was confused most of the times with other activities, while in other studies these transitions would not even be possible. Would we remove those transitions from the confusion matrices, accuracy for those classes rises to comparable levels as other reported literature.

## 4.2 Limitations

The ultimate goal of the developed algorithms is to use them in a prosthetic device. However, only able-bodied subjects were measured. This could be seen as a user with a best case scenario prosthesis. Therefore, it is important to validate the intent recognition algorithms to see how they work in general and to see its effectiveness. The amputee must have an active prosthesis, i.e. actuated, as walking with a passive device does not represent similar muscle activation and kinematics as in healthy subjects.

Another limitation concerning the subject population is that the subjects were relatively young and activity level was high, therefore, one could argue that it is not representative for the targeted amputee population. However, the MyLeg prosthesis is targeted for an amputee with a K level of 3-4, i.e. the active adult and most active amputees are relatively young [33], which makes the subject population somewhat representative in terms of age and activity.

The measurement set-up was a limited way of utilizing multi-array EMG. Multi-array EMG is mostly used for motor neuron decomposition [4] when measured in a limited area or in areas with a high density of different muscles, e.g. the forearm. As decomposition was not the aim of this study and the density of muscles was low, one could argue that one bipolar channel per muscle would have been sufficient and therefore, redundancy of data was collected. However, this set-up was aimed to be used in amputee subjects, where locating the muscle of interest is difficult. This data enables us to look at different leads within the grid, to find an optimal electrode configuration, which might be very helpful for an amputee population. Thus, although the usage of multi-array EMG in this thesis was limited, interesting follow-up studies on electrode configuration can be conducted with the collected data.

All algorithms were trained on data which contained data from the same subject during the same measurement. Although the algorithms were trained with random samples of the data and thus were unable to memorize the complete sequence, it remains to be seen how well the algorithms perform during a different day. Therefore, additional measurements should be performed, where a subject

performs a similar protocol on three different measurement days, to validate the robustness of the algorithms. As the measurement system is completely wearable, validation in a home environment is feasible as well and would give good insight in the capabilities of the algorithms in real-life.

The features used in the feature engineering method are described over two decades ago by Hudgins *et al* [22] and interestingly enough no physiological explanation has been given. It seems that most studies in literature use features because ‘they work’ and no longer think of ‘why they work’. Phinyomark *et al* investigated 85 different features to find an optimal feature set for upper limb control [34]. None of these additional features made it to the feature set selected by Hu *et al*, which only used the features selected by Hudgins *et al* plus an autoregressive model, which was used by Huang *et al* in 2005 [23] for prosthetic control. It is strongly advised to investigate additional features for lower limb control as current features could be regarded as out-dated, find an optimal feature set with e.g. genetic algorithms [35] and explain why they work.

### 4.3 Future Outlook

The data set contained many different types of activities which enables research possibilities on gait related studies using kinematics and/or EMG. All trained algorithms can be implemented in a prosthetic device. In terms of IMU placement, in principle all IMUs can be attached to the prosthesis, without the need of additional kinematic sensors on the patient itself. The motor encoders within the prosthetic leg can measure knee and ankle angle and gait events can accurately be determined using force sensors or IMUs within the foot or shank [36]. Kinetics were not collected in this study due to the difficulty of measurement outside a lab environment, but force and torque sensors within a prosthesis could provide additional data for intent recognition.

This data set was manually labeled, which was time consuming. Fully preparing data of one subject could take over five hours. Another study could be investigating the possibilities of automatic labelling, to enable even longer measurements, without the need for manual labour. This is the domain of human activity recognition on which many studies have been performed as well [16, 17, 28]. The current data set contained various subjects and various possible labels, which makes it a challenging data set for activity recognition.

Current state of the art in deep learning for image recognition are very deep models, i.e. models with many layers. Those were trained on massive data sets consisting of many classes of images. However, when such data sets are not available, for instance because it is very time consuming to collect the data or not feasible to collect the data, deep learning could not show its potential. Interestingly enough, using a trained model for a image classification task and retrain it on a small data set in a completely different field could result in a better performance, than training a model from scratch [37]. For instance a study by Johnson *et al* [38] showed that they were able to estimate 3D ground reaction forces from motion capture data by retraining CaffeNet, a model that was training on millions of images. Their training set only consisted of several hundreds of trials from various subjects, but they have managed to reliably estimate ground reaction forces. This suggests that transfer learning is a powerful method which could be employed in upcoming studies on the collected data set.

As stated before, the use of multi-array EMG in this thesis was limited. The electrodes were placed with a relatively high density compared with the total surface area of the upper leg. Therefore, using a relatively low density of uniformly distributed electrodes, covering most of the leg could help to give new insights in intent recognition. In this way, EMG is measured in a non-traditional manner, but patterns of muscle activation of various muscles could be mapped. This is already done in upper limb prosthetic control [39] and shows promising results with the ease of utilizing the set-up.

## Chapter 5

# Conclusion

This study had the following goals: First, to see whether using multi-array EMG outperforms using bipolar EMG in a kinematic driven algorithm for human motor intent recognition and whether EMG has added benefit at all in terms of performance. Secondly, whether feature learning outperforms feature engineering in terms of motor intent recognition. The goal was to come up with algorithms that could readily be applied to a prosthesis user, thus using only kinematic information that could be available from sensors within a prosthesis. It can be concluded that using bipolar EMG and kinematics is the best approach in the described set-up in terms of overall ( $p < 0.001$ ) and transition performance ( $p < 0.0001$ ). However, the added benefit of EMG is small compared with algorithm trained on kinematics only. The developed feature engineering algorithm outperforms feature learning in terms of transition ( $p < 0.0001$ ), but the opposite is true for steady-state performance ( $p < 0.0001$ ). With this research we have gained insight in the possibilities of using EMG and unilateral kinematics to develop an intent recognition system based on machine learning. The feature engineering algorithm based on bipolar EMG and kinematics can easily be implemented in a prosthetic device.



# Appendix A

## Synchronization of EMG and Motion Data

The choice for Xsens over other kinematic modalities, such as Vicon, has been made for several reasons. One, the marker placement of Vicon takes skill and time to set up, where as Xsens is set up with limited effort. Second, the measurement volume of Xsens is one of the largest compared with other modalities. Lastly, on body recordings give the freedom to perform measurements in real-life scenarios and inertial sensors do not suffer the same issues as optic markers, such as lighting [40]. However, there is a major drawback as well, which is the synchronization of Xsens with other modalities. Xsens does not allow to record additional analog signals and only provides recognition of a start and end pulse. If, for whatever reason, one of the pulses is lost, the data becomes difficult to synchronize. This is because it becomes unclear when measuring begins or if there is a time-drift between the two modalities. Therefore, it is preferable to have a continuous synchronization method. Such a method can be based on cross-correlation.

Cross-correlation is a measure of similarity between two functions expressed as the shift in time of one function relative to the other [41]. Let  $f(t)$  and  $g(t)$  denote two signals in time. The cross-correlation ( $R$ ) is defined as:

$$R_{fg}(\tau) = \int_{-\infty}^{\infty} f(t)g^*(t - \tau)dt \quad (\text{A.1})$$

Herein is  $\tau$  the time lag or shift in time. Maxima and minima in the cross-correlation denote where the two signals are most positively or negatively correlated. This property makes the cross-correlation function commonly used in pattern recognition, as it becomes possible to find similarities between a sample (or pattern) and another signal.

In this section we describe a custom synchronization method based on an additional accelerometer using cross-correlation. In our case it is assumed that the additional accelerometer placed on top of the Xsens IMU will measure similar acceleration, thus it can be used to match the two signals.

### A.1 Methods

#### Experimental set up

Seven able bodied subjects (three male, four female) participated in this part of the study. Subjects were  $23 \pm 2$  years,  $177 \pm 13$  cm tall and weighed  $71 \pm 11$  kg. All subjects declared not to have any gait impairments at the time of the measurements and completed the following protocol in April 2019.

Two devices need to be synchronized: the MVN Link suit (Xsens, Enschede, The Netherlands), which was sampled at 240Hz, and the Sessantaquattro (Bioelettronica, Turin, Italy), sampled at

2000Hz, which were used to measure kinematics and EMG respectively. The auxiliary port of the Sessantaquattro enabled to measure 2D accelerations at 2000Hz, using the ADXL337 (Analog Devices, Norwood, MA, USA). The accelerometer was placed on top of the Xsens IMU on the right thigh of the subject. The next step was to use a secondary synchronization to validate the accelerometer based synchronization. This secondary synchronization was based on sound. The subject performed a movement which made sound and involved acceleration, i.e. kicking against a metal cylinder, and the sound was recorded via the EMG channels of the Sessantaquattro, using SRS-5 speakers (Sony, Tokyo, Japan). The speakers were placed within ten centimeter from the cylinder. Schematic outline of the set-up can be seen in figure A.1. It was assumed that both systems are synchronized internally. Hereafter the subject walked to a chair, sit down, stood up and walked back and kicked the metal cylinder again. This measurement was repeated three times.

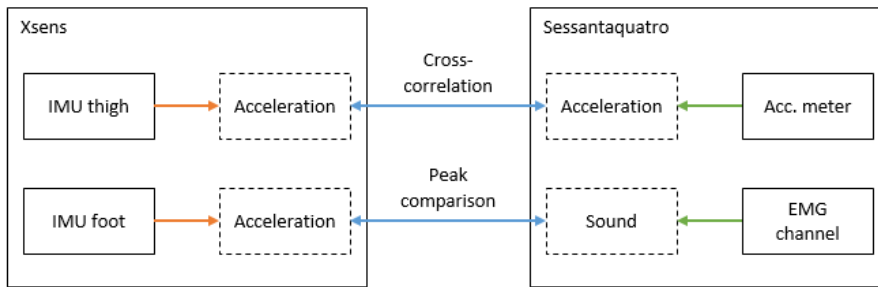


**Figure A.1:** Schematic outline of the measurement set-up. From the IMUs of Xsens the acceleration is taken and compared with the acceleration from the additional accelerometer and sound recorded using an EMG channel of the Sessantaquattro using two different methods: one based on cross-correlation and one based on peak detection.

## Data processing

Data processing was performed in python 3.6. As the kick was performed with the foot, acceleration data from the foot showed the moment of hitting the metal cylinder most clearly. This moment was used to compare it with the measured sound of the kick. The moment of impact was defined as the peak acceleration in the direction of the kick measured by the foot accelerometer and the exceeding of a threshold for sound, see figure A.2. The difference between the time stamps of the moment of impact in the two signals was the estimated time shift for this method.

The acceleration of the right thigh measured by the Xsens IMU and the additional accelerometer were compared using cross-correlation. Based on peaks in the knee angles, segments of activities of interest were extracted from the Xsens data with an eight second window size, e.g. see figure A.3a. Those segments were resampled to 1000Hz and filtered with a zero-lag band pass filter with cut-off frequencies of 0.1 and 120 Hz. The gravity component of the additional accelerometer is removed using a zero-lag high pass filter at 0.1 Hz and hereafter the acceleration was filtered with a 120 Hz zero-lag low pass filter. As the lowest sample frequency of the two systems is 240Hz, both signals are filtered using a 120Hz filter to prevent aliasing. All filters are second order butterworth filters.

The filtered Xsens segments were cross-correlated with the filtered acceleration from the additional accelerometer, see figure A.3b. Peaks in the absolute cross-correlation were determined using a peak finding algorithm. Using the absolute cross-correlation avoided the need to flip one of the acceleration signals if one of accelerometers was placed upside down. The location of the highest peak was the estimated time shift between the two signals for the cross-correlation based method.

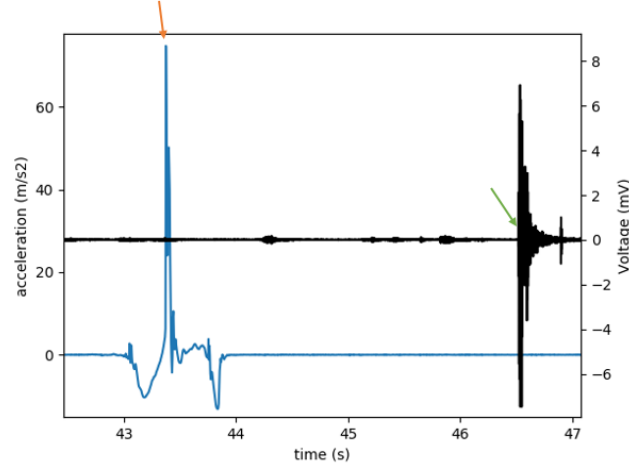


**Figure A.2:** Foot acceleration (blue) and recorded sound (black) using the left and right y-axis respectively. The orange arrow indicates the moment of impact in the acceleration and green arrow indicates the impact in sound.

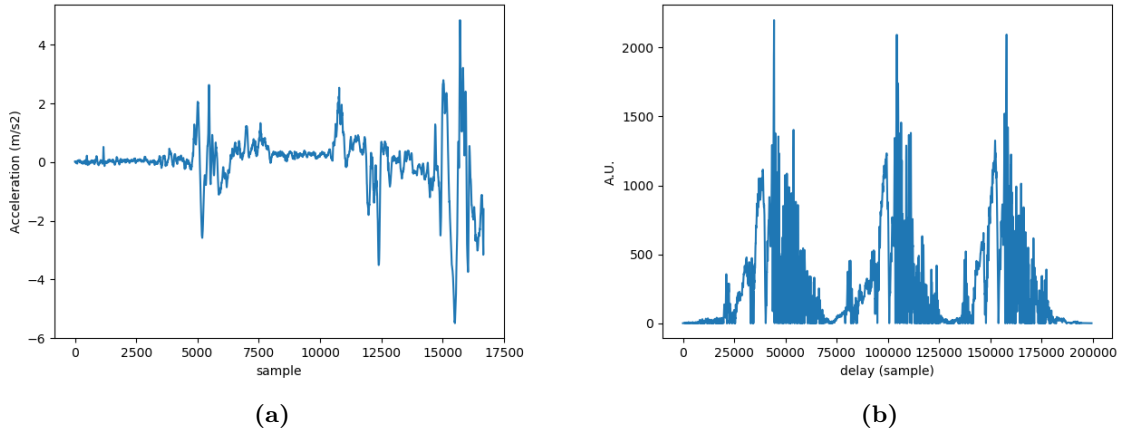


**Figure A.3:** (a) Sample of Xsens thigh acceleration during stand-to-sit-to-stand and a first step, resampled at 2000Hz. (b) Cross-correlation of the Xsens sample with the acceleration from the additional accelerometer. It can be seen clearly that the measurement has been repeated three times. Highest peak corresponds with the estimated delay.

The cross-correlation was determined for a window of eight seconds around two different activities: stand-to-sit-to-stand and walking. The difference between estimated delay of each method were determined for each trial and these differences are averaged per subject. A Wilcoxon signed rank test was used to determine significance.

## A.2 Results

Results are shown in table A.1. Average time difference between the two methods was  $-0.24 \pm 2.03$  ms using sit-to-stand-to-sit and  $-0.06 \pm 1.10$  ms using walking data, which were both not significant ( $p > 0.1$ ). The sample rate of Xsens was 240Hz, which corresponded to a sample time of 4.166 ms. Thus the found time difference is within the sample time of Xsens. There is also no significant difference between using sit-to-stand-to-sit and walking data ( $p > 0.1$ ).

**Table A.1:** Average differences  $\pm$  standard deviation in estimated delay between each method for two movements: stand-to-sit-to-stand (sit-stand) and walking. The results are reported per subject and an average over all subjects is reported as well. Subject 1 did not perform the walking tests during the measurement.

Subject	Sit-stand (ms)	Walking (ms)
1	$1.57 \pm 0.17$	NA
2	$1.56 \pm 1.93$	$0.06 \pm 1.09$
3	$-2.09 \pm 1.15$	$0.99 \pm 1.69$
4	$-0.94 \pm 1.58$	$-0.5 \pm 0.45$
5	$-2.37 \pm 1.41$	$-0.30 \pm 1.59$
6	$-2.27 \pm 0.98$	$-1.98 \pm 0.63$
7	$2.90 \pm 0.17$	$1.41 \pm 0.61$
<b>Average</b>	<b><math>-0.24 \pm 2.03</math></b>	<b><math>-0.06 \pm 1.10</math></b>

### A.3 Discussion

Time shift between the two methods fall within the sample time of the modality with the lowest sample frequency. This suggests that the resolution of the method is adequate to be used for synchronization and a synchronization pulse should no longer be necessary. There are a few points for consideration.

Two activities were used to determine the resolution of the method, sitting-standing and walking. These results suggest it does not matter which activity is performed, as the time shift is not significantly different. Therefore, one can assume that this method can also be used for other activities, such as ascending stairs. Important is that the activity needs to involve movement of the thigh in the sagittal plane, or else no acceleration is measured. Placement on other body segments is not investigated in this research, however, it can be expected that the method will perform equally well. This can be expected because the acceleration of movements is similar enough to be used for synchronization if two sensors are placed on top of each other.

The measurement duration is relatively short (two minutes) compared with the total measurement time (up to one hour). It remains to be seen whether the synchronization method could still reliably determine the shift if the time deviation becomes too large between the two measurement systems. As the performed activities are cyclic, it can happen that a shift of one cycle could occur. This can be overcome by using longer signals for correlation.

The assumption is made that the measured sound is instantaneous. This is not completely true, as sound travels with around 3 ms per meter. Therefore, the speakers had to be placed close to the metal cylinder. As the distance from the speaker to the cylinder is around ten centimeter, the average delay induced by the speed of sound is 0.3 ms, thus negligible. A light-based system could also be used, which might be even more accurate, although a higher accuracy in this case should not be necessary.

Lastly, there is one other item of consideration. Using other kinematic data from Xsens, such as knee angles, activities of interest can be extracted automatically. E.g. it is relatively easy to recognize sitting and standing movements. In this way the synchronization is automated and will reduce time required to synchronize by the analyst. Various points of interest could be selected in the data, to re-synchronize the data regularly, to optimize performance.

### A.4 Conclusion

The custom synchronization method based on acceleration cross-correlation is not significantly different from a sound based synchronization method ( $p > 0.1$ ). The resolution of the method is around

2 ms, which is below the 4 ms sample time of Xsens. Both sit-stand transitions and walking can be used for synchronization. These results suggests that this method is suitable to synchronize Xsens' MVN Link suit and other modalities, such as Bioelettronica's Sessantaquattro.



# Appendix B

## Additional collected data

This section is to give an overview of other data that is collected during my thesis.

### Measurements at University of Twente

The data was collected from ten able-bodied subjects. The study and protocols are carried out in accordance with the approval of the medical ethical review board of Twente with written informed consent from all subjects.

Ten able bodied subjects (seven male, three female) participated in this part of the study. Subjects were  $23 \pm 2$  years,  $184 \pm 10$  cm tall and weighed  $77 \pm 10$  kg. All subjects declared not to have any gait impairments at the time of the measurements and completed the following protocol between December 2018 and January 2019.

Lower body kinematics were collected using a MVN Link suit (Xsens, Enschede, The Netherlands), which uses eight inertial measurement units (IMUs). 3D acceleration, velocity, position as well as 3D angular velocity and position are recorded per segment at a sample frequency of 240Hz. IMU placement and calibration is done according to Xsens guidelines [29].

EMG signals were recorded using bipolar electrodes, eight SC-F03 Sensors and eight SC-F04 Mini Sensors (Delsys, Boston, MA, USA) at a sample frequency of 1000Hz. Eight muscles per leg were recorded: gluteus maximus (Gmax), gluteus medius (Gmed), rectus femoris (RF), vastus lateralis (VL), biceps femoris (BF), semitendinosus (ST), tibialis anterior (TA) and gastronemius medialis (GM). These muscles were chosen as they are responsible for hip, knee and ankle flexion/extension and were also targeted in other studies, e.g. [32]. Electrodes were placed according to the Surface ElectroMyoGraphy for the Non-Invasive Assessment of Muscles (SENIAM) project guidelines [30]. Real-time visualization and recording was done using a in-house written script in MATLAB Simulink. Xsens and EMG were synchronized using an analog pulse to start and stop the recordings.

Measurements were conducted at the Wearable Robotics Lab of the University of Twente, using obstacles constructed for the Cybathlon [42] by the Department of Biomechanical Engineering. Obstacles used were the stairs (rise 17 cm, run 28 cm), ramp with two different slopes (15 and 20 degrees) and uneven terrain consisting of stepping stones on a surface. Forty trials were conducted per subject. A trial consisted of sitting (S), standing (St), walking (W), stair ascent(SA)/descent(SD), ramp ascent(RA)/descent(RD), walking on uneven terrain (UT) and walking in confined spaces (CS). As the ramp had two different slopes two different trials were conducted, twenty each:

- S→St→W→SA→SD→W→RA(20)→W→RD(15)→W→UT→CS→W→St→S
- S→St→W→RA(15)→W→RD(20)→W→SA→SD→W→CS→UT→W→St→S

Confined spaces consisted of walking small steps in eight different directions, e.g. side step left, diagonal step right backwards, etc. Subjects walked in their own preferred speed and after ten trials a

## APPENDIX B. ADDITIONAL COLLECTED DATA

---

small break was administered to avoid fatigue and check sensor placement. Each trial had a duration of around 1 minute 15 seconds. Total measurement time including subject preparation, sensor placement and calibration was around two hours.

# Bibliography

- [1] V. Kooiman, H. Van der Meet, N. Verdonschot, T. Fridriksson, K. Lechler, M. Oddsson, E. G. Olafsdottir, F. Thorsteinsson, E. Prinsen, E. Van Staveren, and R. Carloni, “Deliverable D2.1 Amputees’ requirements.” [cordis.europa.eu/project/rcn/213177](http://cordis.europa.eu/project/rcn/213177), 2018.
- [2] R. Carloni, “MyLeg: Smart and intuitive osseointegrated transfemoral prostheses embodying advanced dynamic behaviors.” [MyLeg.eu](http://MyLeg.eu), 2018.
- [3] H. A. Varol, F. Sup, and M. Goldfarb, “Multiclass real-time intent recognition of a powered lower limb prosthesis,” *IEEE Transactions on Biomedical Engineering*, vol. 57, no. 3, pp. 542–551, 2010.
- [4] R. Merletti and D. Farina, *Surface Electromyography : Physiology, Engineering, and Applications*. Hoboken, New Jersey: John Wiley & Sons, Inc., 4 2016.
- [5] A. Phinyomark and E. Scheme, “EMG Pattern Recognition in the Era of Big Data and Deep Learning,” *Big Data and Cognitive Computing*, vol. 2, no. 3, p. 21, 2018.
- [6] E. C. Wentink, V. G. Schut, E. C. Prinsen, J. S. Rietman, and P. H. Veltink, “Detection of the onset of gait initiation using kinematic sensors and EMG in transfemoral amputees,” *Gait and Posture*, vol. 39, no. 1, pp. 391–396, 2014.
- [7] R. Fluit, E. Prinsen, S. Wang, and H. Van Der Kooij, “A comparison of control strategies in commercial and research knee prostheses,” *IEEE Transactions on Biomedical Engineering*, vol. 9294, no. c, pp. 1–1, 2019.
- [8] A. J. Young, T. A. Kuiken, and L. J. Hargrove, “Analysis of using EMG and mechanical sensors to enhance intent recognition in powered lower limb prostheses,” *Journal of Neural Engineering*, vol. 11, no. 5, 2014.
- [9] A. J. Young and L. J. Hargrove, “A Classification Method for User-Independent Intent Recognition for Transfemoral Amputees Using Powered Lower Limb Prostheses,” *IEEE Transactions on Neural Systems and Rehabilitation Engineering*, vol. 24, no. 2, pp. 217–225, 2016.
- [10] J. Ryu and D. H. Kim, “Real-time gait subphase detection using an EMG signal graph matching (ESGM) algorithm based on EMG signals,” *Expert Systems with Applications*, vol. 85, pp. 357–365, 2017.
- [11] S. Huang, J. P. Wensman, and D. P. Ferris, “Locomotor Adaptation by Transtibial Amputees Walking with an Experimental Powered Prosthesis under Continuous Myoelectric Control,” *IEEE Transactions on Neural Systems and Rehabilitation Engineering*, vol. 24, no. 5, pp. 573–581, 2016.
- [12] B. H. Hu, E. J. Rouse, and L. J. Hargrove, “Using bilateral lower limb kinematic and myoelectric signals to predict locomotor activities: A pilot study,” *International IEEE/EMBS Conference on Neural Engineering, NER*, pp. 98–101, 2017.

- [13] B. Hu, E. Rouse, and L. Hargrove, "Fusion of Bilateral Lower-Limb Neuromechanical Signals Improves Prediction of Locomotor Activities," *Frontiers in Robotics and AI*, vol. 5, p. 78, 6 2018.
- [14] D. C. Tkach and L. J. Hargrove, "Neuromechanical sensor fusion yields highest accuracies in predicting ambulation mode transitions for trans-tibial amputees," *Proceedings of the Annual International Conference of the IEEE Engineering in Medicine and Biology Society, EMBS*, pp. 3074–3077, 2013.
- [15] J. A. Spanias, A. M. Simon, K. A. Ingraham, and L. J. Hargrove, "Effect of additional mechanical sensor data on an EMG-based pattern recognition system for a powered leg prosthesis," *International IEEE/EMBS Conference on Neural Engineering, NER*, vol. 2015-July, pp. 639–642, 2015.
- [16] F. Ordóñez and D. Roggen, "Deep Convolutional and LSTM Recurrent Neural Networks for Multimodal Wearable Activity Recognition," *Sensors*, vol. 16, p. 115, 1 2016.
- [17] J. Wang, Y. Chen, S. Hao, X. Peng, and L. Hu, "Deep learning for sensor-based activity recognition: A survey," *Pattern Recognition Letters*, vol. 119, pp. 3–11, 3 2019.
- [18] C. D. Hoover, G. D. Fulk, and K. B. Fite, "Stair ascent with a powered transfemoral prosthesis under direct myoelectric control," *IEEE/ASME Transactions on Mechatronics*, vol. 18, no. 3, pp. 1191–1200, 2013.
- [19] O. A. Kannape and H. M. Herr, "Volitional control of ankle plantar flexion in a powered transtibial prosthesis during stair-ambulation," *2014 36th Annual International Conference of the IEEE Engineering in Medicine and Biology Society, EMBC 2014*, pp. 1662–1665, 2014.
- [20] A. Phinyomark, P. Phukpattaranont, and C. Limsakul, "Feature reduction and selection for EMG signal classification," *Expert Systems with Applications*, vol. 39, no. 8, pp. 7420–7431, 2012.
- [21] H. F. Nweke, Y. W. Teh, M. A. Al-garadi, and U. R. Alo, "Deep learning algorithms for human activity recognition using mobile and wearable sensor networks: State of the art and research challenges," *Expert Systems with Applications*, vol. 105, pp. 233–261, 2018.
- [22] B. Hudgins, P. Parker, and R. Scott, "A new strategy for multifunction myoelectric control," *IEEE Transactions on Biomedical Engineering*, vol. 40, no. 1, pp. 82–94, 1993.
- [23] Y. Huang, K. B. Englehart, B. Hudgins, and A. D. Chan, "A Gaussian mixture model based classification scheme for myoelectric control of powered upper limb prostheses," *IEEE Transactions on Biomedical Engineering*, vol. 52, no. 11, pp. 1801–1811, 2005.
- [24] L. Hargrove, K. Englehart, and B. Hudgins, "A training strategy to reduce classification degradation due to electrode displacements in pattern recognition based myoelectric control," *Biomedical Signal Processing and Control*, vol. 3, pp. 175–180, 4 2008.
- [25] T. Stiefmeier, D. Roggen, G. Ogris, P. Lukowicz, and G. Tr, "Wearable Activity Tracking in Car Manufacturing," *IEEE Pervasive Computing*, vol. 7, pp. 42–50, 4 2008.
- [26] H. Sagha, S. T. Digumarti, J. del R. Millan, R. Chavarriaga, A. Calatroni, D. Roggen, and G. Troster, "Benchmarking classification techniques using the Opportunity human activity dataset," in *2011 IEEE International Conference on Systems, Man, and Cybernetics*, pp. 36–40, IEEE, 10 2011.

- 
- [27] A. Reiss and D. Stricker, “Introducing a New Benchmarked Dataset for Activity Monitoring,” in *2012 16th International Symposium on Wearable Computers*, pp. 108–109, IEEE, 6 2012.
- [28] Y. Guan and T. Plötz, “Ensembles of Deep LSTM Learners for Activity Recognition using Wearables,” *Proceedings of the ACM on Interactive, Mobile, Wearable and Ubiquitous Technologies*, vol. 1, pp. 1–28, 6 2017.
- [29] Xsens, “Xsens MVN Analyze - Products.” [xsens.com/products/xsens-mvn-analyze/](https://xsens.com/products/xsens-mvn-analyze/).
- [30] H. J. Hermens, B. Freriks, R. Merletti, D. Stegeman, J. Blok, G. Rau, C. Disselhorst-Klug, and G. Hägg, “SENIAM - Deliverable 8 - European Recommendations for Surface ElectroMyoGraphy Chapter,” pp. 8–11, 1999.
- [31] F. Chollet *et al.*, “Keras.” [keras.io](https://keras.io/), 2015.
- [32] B. Hu, E. Rouse, and L. Hargrove, “Benchmark Datasets for Bilateral Lower-Limb Neuromechanical Signals from Wearable Sensors during Unassisted Locomotion in Able-Bodied Individuals,” *Frontiers in Robotics and AI*, vol. 5, no. February, pp. 1–5, 2018.
- [33] M. Yilmaz, D. Gulabi, I. Kaya, E. Bayram, and G. S. Cecen, “The effect of amputation level and age on outcome: an analysis of 135 amputees,” *European Journal of Orthopaedic Surgery & Traumatology*, vol. 26, pp. 107–112, 1 2016.
- [34] A. Phinyomark, R. N. Khushaba, E. Ibáñez-Marcelo, A. Patania, E. Scheme, and G. Petri, “Navigating features: a topologically informed chart of electromyographic features space,” *Journal of The Royal Society Interface*, vol. 14, p. 20170734, 12 2017.
- [35] E. P. Ijjina and K. M. Chalavadi, “Human action recognition using genetic algorithms and convolutional neural networks,” *Pattern Recognition*, vol. 59, pp. 199–212, 11 2016.
- [36] H. F. Maqbool, M. A. B. Husman, M. I. Awad, A. Abouhossein, P. Mehryar, N. Iqbal, and A. A. Dehghani-Sanij, “Real-time gait event detection for lower limb amputees using a single wearable sensor,” in *2016 38th Annual International Conference of the IEEE Engineering in Medicine and Biology Society (EMBC)*, pp. 5067–5070, IEEE, 8 2016.
- [37] K. Weiss, T. M. Khoshgoftaar, and D. Wang, “A survey of transfer learning,” *Journal of Big Data*, vol. 3, p. 9, 12 2016.
- [38] W. R. Johnson, A. Mian, C. J. Donnelly, D. Lloyd, and J. Alderson, “Predicting athlete ground reaction forces and moments from motion capture,” *Medical & Biological Engineering & Computing*, vol. 56, pp. 1781–1792, 10 2018.
- [39] D. Yang, Y. Gu, R. Liu, and H. Liu, “Dexterous motion recognition for myoelectric control of multifunctional transradial prostheses,” *Advanced Robotics*, vol. 28, pp. 1533–1543, 11 2014.
- [40] D. Roetenberg, H. Luinge, and P. Slycke, “Xsens MVN: Full 6DOF human motion tracking using miniature inertial sensors,” *Xsens Motion Technol. BV Tech Rep*, vol. 3, pp. 1–9, 2013.
- [41] S. Haykin and M. Moher, *An Introduction to Analog and Digital Communications*. Wiley Textbooks, 2012.
- [42] ETH Zurich, “Cybathlon 2016.” [www.cybathlon.ethz.ch](http://www.cybathlon.ethz.ch), 2016.